Chapter 3

Photogrammetric Survey in Volcanology: A Case Study for Kamchatka Active Volcanoes

Viktor Dvigalo, Alina Shevchenko and Ilya Svirid

Additional information is available at the end of the chapter

http://dx.doi.org/10.5772/63577

Abstract

The photogrammetric method has been used to study active volcanoes in Kamchatka for more than 100 years. It is still the most effective method for consistently monitoring short-term changes in the morphology of volcanic structures and for obtaining accurate parameters of eruptions. This chapter shows the specific features of photogrammetry application in volcanological research and development of this method in the context of investigating Kamchatkan volcanoes. We also present the results of the study of volcanic objects with various morphologies, composition, and types of activity with regard to the specific features of the 2001–2012 growth of the dome at Molodoy Shiveluch Volcano, the effects of the 1975–1976 Great Tolbachik Fissure Eruption and of the 2012–2013 Tolbachik Fissure Eruption, the morphodynamics of Troitsky Crater on Maly Semyachik Volcano, and the morphological changes of Akademii Nauk Caldera after the catastrophic 1996 eruption. The chapter shows the way forward for the development of the photogrammetric method in volcanology.

Keywords: Kamchatkan active volcanoes, photogrammetry, lava dome, fissure eruption, volcanic lake, collapse caldera

1. Introduction

Photogrammetry is a branch of science at the junction of optics, mathematics, and photography, which is aimed at the identification of objects' shapes, sizes and locations using photographic images. Photogrammetric method is necessary in all branches of the natural sciences for obtaining objects' morphometric characteristics in cases when it is easier to take a photograph than to measure directly, e.g., in studying such complex and dangerous objects as volcanoes.

The photogrammetric method allows for the measurement of short-life or even moving objects and could be useful in determining geometric forms, sizes, and velocities of eruptive products, such as eruptive clouds, lava, and pyroclastic flows.

Photogrammetric investigations have been used in volcanology for more than a century. At the present time, there are many methods for remote sensing, such as airborne laser scanning or satellite radar and interferometry. Nevertheless, photogrammetry is still of great importance. It is cheaper and more universal than all other remote methods of measurement. In addition, the photogrammetric method could be used to process archival aerial photographs from conventional cameras as well as satellite stereoscopic images.

For a long time, the photogrammetric approach remained rare in volcanology, mainly due to the high cost of equipment and the complexity of the work. Lately, thanks to technological advances, photogrammetric studies have become more accessible. The increase in quality of conventional digital cameras makes it possible to use them for this purpose. The photogrammetric processing of images on the computer eliminates the need for expensive optical–mechanical equipment. Thus, the development of digital image processing caused the increase of interest in photogrammetry for volcanological investigations.

2. The sequence of photogrammetric works

A large number of special works refer to photogrammetric theory (see e.g. reference [1]). Therefore, we just briefly describe the method itself and some of the special characteristics of its application in volcanology. Concrete and practical recommendations depend on hardware and software, which is why we provide only the very general information necessary for understanding the essence and planning of photogrammetric investigations.

Photogrammetric work consists of four stages:

1. Geodetic preparatory work in situ;
2. Photo survey with all technological requirements;
3. Photogrammetric processing of images;
4. DTM plotting.

2.1. Geodetic preparatory work

During this stage of fieldwork, the ground control points are placed down on the surface of the object and their coordinates are defined for geodetic reference of further photogrammetric models. The ground control points are placed so that subsequently they can be easily identified in aerial photographs. This stage is the most laborious and expensive, but some tricks could be used to solve this problem. Thus, when a single object will be investigated over a number of years, this stage only needs to be performed once. After that, we can choose a georeferenced photogrammetric model with easily detected points that do not change their location over time

http://dx.doi.org/10.5772/63577

(e.g., rocks' tops, dykes, and large stones that are not on the slopes). We can then use their coordinates for the absolute orientation of all other models. This could be used not only to process images obtained after establishing the geodetic basement but also to process images that were made before. It can therefore be useful when working with archival images.

Though this method of orientation can result in the possible loss of absolute accuracy for the photogrammetric model, it has a rather high relative accuracy. Taking into account the alteration of the object's surface (e.g., when a crater is formed or filled with lava, pre- or posteruptive deformations of the earth's crust) is very essential for volcanological investigations, and so in most cases, in using the photogrammetric model one should choose relative rather than absolute accuracy. In the most difficult cases, for example, when the erupting volcano is investigated and geodetic work in the area is dangerous, absolute orientation could be made by points identified on topographic maps, if available.

2.2. Aerial photography

Stereophotogrammetric investigations provide the most accurate information about an object. To measure the parameters of the object, these investigations use stereoscopic photography. Stereoscopic images are obtained by shooting an object from different angles. The distance between the survey points is called a basis.

Volcanoes rise steeply above the surrounding terrain and also could pose a hazard during ground investigations, so the photography for photogrammetric purposes is better done from the air. Aerial photography using an analogue or digital camera usually requires a specially equipped air vehicle with a hatch in the floor of the cabin as well as an onboard operator. However, modern digital cameras meet the requirements for the photogrammetric investigation of volcanoes, and they are compact enough for both aerial camera mounting and handheld shooting.

Shooting for a photogrammetric survey can also be carried out using a nonindustrial professional camera. That camera must be equipped with a fixed-focus lens, and autofocus must be switched off. The camera can be calibrated either before or after shooting, but the focal length of the camera and the lens position should not be changed between calibration and shooting.

As a rule, for an aerial survey, the camera is directed vertically downward, and in this case, aerial images are called vertical. If the angle of deviation from the vertical is more than 5°, then this is an oblique aerial photographic survey.

Aerial photography for stereophotogrammetric processing has its own peculiarities. The same part of the object's surface should be shown on at least two frames. If the resolution of the camera or the flight altitude restriction does not allow for a stereo pair of images to be obtained with complete and detailed capturing of the object and the ground control points, then strip or block photography is used. For this type of survey, it is essential that some part of the object's surface (it does not matter which) should be captured in three images of the same strip; this is necessary for the creation of a continuous stereo model. Consequently, the overlap area of two adjacent frames in the strip should be at least 55% of the frame area. The block consists of

several strips with mutual side overlap of the object images. This overlap could be not so large and comprises 15–30% of the frame area.

It should be noted that the relative height of the volcanic edifice can be almost the same as the altitude of the aerial survey flight. As a result, there may be significantly less overlap for images of the object's higher-altitude surfaces than for its lower-altitude ones. To keep constant overlapping, we must correct the inter-frame time interval even in the process of surveying a single pass, reducing it when shooting the top part of the volcano, and increasing it when shooting the foot of the volcano.

2.3. Image processing

Regardless of the equipment and software used, the photogrammetric processing of images consists of the following stages:

1. Interior orientation of images;
2. Relative orientation of images;
3. Exterior orientation of the stereo model.

Interior orientation refers to the camera's geometric parameters: the exact focal length, frame size, main point position (i.e., point of the frame in front of the optical centre of the lens), and the lens radial distortion coefficients. All of these parameters can be obtained from the camera's calibration. In the case of analogue aerial cameras, one should also specify the position of fiducial marks or the distance between them in the frame. Fiducial marks are images of special elements in the film plane of analogue cameras, defining a system of rectangular coordinates for each image.

Relative orientation is made to combine the images into a free photogrammetric model (or stereo model), which is a set of images with the data on the relative camera location for each moment of photography. These include the data on angular position (i.e., angle of inclination and rotation) and spatial position (i.e., length and direction of the base) of the camera from frame to frame. They can either be received from sensors used for surveying (e.g., tiltmeters, gyroscopes, statoscope, GPS sensors) or calculated on the basis of the images. The last variant requires a set of corresponding points in six generally located zones in the overlapping areas of images in each stereo pair. Most photogrammetric software can find these points automatically. The accuracy of the detection of relative orientation parameters from images is generally higher than the data from sensors.

Exterior orientation establishes a correspondence of the photogrammetric model's spatial coordinates to the geodetic coordinates in the area of the object. The exterior orientation of photogrammetric models resulting from one stereo pair of images requires a minimum of three points with known geodetic coordinates that are not located on a one line. In the case of strip photo surveys, it is necessary to have two reference points at each end of the pass, and preferably at least one reference point in the middle. Block photo surveys require reference points at the corners of the shot area and a certain middle point. To exclude rough defects, one should have verification points with exact geodetic coordinates in addition to the minimum

http://dx.doi.org/10.5772/63577

number of reference points. It is good if quantity of verification points is equal to reference points. In the result of an association between the model calculated and the actual coordinates of the verification points, we can define horizontal and vertical errors.

Exterior orientation using GPS coordinates is possible, but it is not recommended to use only this method for aerial survey. The accuracy of surveying point coordinates obtained in flight is not high. Setting the coordinates in flight can result in their shifting along the flight line due to delays in their recording. Besides, all surveying points are on the flight line, which is usually nearly straight, and in such cases, it is practically impossible to make complete exterior orientation. The errors of such orientation may reach up to 10 m or more.

In case of the stereophotogrammetric processing of satellite images, the rational polynomial coefficient (RPC) model is typically used, the coefficients of which, accompanying the images, implicitly include all the necessary parameters of the interior, relative, and exterior orientation. Unfortunately, satellite stereo images often do not meet the requirements for the morphometric investigation of volcanoes. We need images with a spatial resolution of 1 m per pixel or higher to have good mapping of the topography changes associated with volcanic activity.

2.4. DTM plotting

After orientation, the photogrammetric model can easily provide the geodetic coordinates of any point on the object's surface. They can be plotted manually by adjusting marks on the image of the object's surface displayed on a stereo monitor (or by using a common monitor coupled with anaglyph glasses). However, a large number of points makes such processing difficult, thus the majority of photogrammetric processing software is capable of automatic point matching. The algorithms used in such software are based on scanning the images for unique objects with their subsequent matching in various images.

Unfortunately, the volcanic landscape has a set of features that complicates the algorithmic processes. These include steep slopes; texture zones that can easily be recognized in one image but can become faded in the next image; uniform surfaces, such as surfaces covered with scoria or snow with no unique objects; and steam and gas-and-ash emissions, which hide the surface from the camera lens. All of these peculiarities complicate automatic processing, which results in large errors during DTM plotting. Consequently, the software must support visual control to provide possibility of manual correction of automatically determined points within a stereo model.

The matching results in a point cloud, which is then transformed into DSM and subsequently into DTM. Fortunately, the active volcanoes on Kamchatka are barely covered with vegetation, thus the majority of DSM are equal to DTM.

The obtained DTM becomes a basis for the final materials. These may include maps, orthophotomaps, three-dimensional (3-D) pictures both in representative colours and, if available in the software, texturized from original photographs. Moreover, DTM allows for all necessary measurements to be taken, including volume measurements of solid deposits from eruptions, liquid lava, and negative landforms on the volcanic edifices. Such measurements require software that can compare the surfaces of two DTMs and measure the volume between them.

3. History of photogrammetric surveys in Kamchatka

3.1. The 1908–1910 Kamchatka expedition of the Russian Geographic Society

The photogrammetric method was used for the first time during the investigation of the Kamchatkan volcanoes in 1908–1910 by N. G. Kell and other members of the geological department of the Kamchatka expedition of the Russian Geographical Society [2–4]. One of the primary tasks set before the geological department was to study the forms, sizes, and locations of the volcanoes, so the scientists chose the theodolite triangulation method (**Figure 1**) and terrestrial photogrammetry. During the summer of 1908, the members of the expedition used conventional cameras. During the winter of 1908–1909, they constructed a "photogrammeter" using an Ernemann camera, parts from a surveyor's table, and an alidade. In spring 1910, the Laussedat phototheodolite was transported from St. Petersburg to Kamchatka and was used for a panoramic photogrammetric survey of the volcanoes.

Figure 1. N. G. Kell working with theodolite. Photo by S. A. Konradi, 1909.

http://dx.doi.org/10.5772/63577

The investigation resulted in about 2000 single photographs and stereo pairs of almost all of the active volcanoes and many of the dormant ones (**Figure 2**). Some of the stereo pairs, along with the results from the theodolite survey, were used by N. G. Kell for plotting the first map of the Kamchatkan volcanoes.

Figure 2. View of Avachinsky Volcano from the Southeast. Photo by S. A. Konradi, 1909.

3.2. The 1946 volcanological expedition

The head of the Laboratory of Volcanology at the USSR Academy of Sciences, academician A. N. Zavaritsky, launched the volcanological expedition in 1946. The expedition's goals included aerial photography of the most important volcanoes of the Soviet Union. Yu. S. Dobrokhotov, an employee of the Laboratory of Airborne Methods at the USSR Academy of Sciences, was responsible for planning and performing the aerial photography [5]. During the period from August 24 to October 2, 1946, the scientists conducted 10 aerial surveys covering about 9000 km in total and taking 6–7 h. The routes were traced in the way that photographs of each volcano were taken vertically, while the most interesting volcanoes were shot circlewise. Yu. S. Dobrokhotov tried to process the obtained materials photogrammetrically without the geodetic adjustment of the images because a ground geodetic survey had not been conducted before. The survey resulted in the maps of Avachinsky and Maly Semyachik volcanoes being plotted without ground control points, as well as topographic profiles of those volcanoes, also including Krasheninnikov Volcano. Besides, Yu. S. Dobrokhotov for the first time described the important role of photogrammetric investigation in volcanology and developed its basic principles.

3.3. Analogue instrumental stereophotogrammetry, 1973–2008

A new age of photogrammetric investigation of the Kamchatkan volcanoes started in 1973. The collaboration between the Institute of Volcanology and the Novosibirsk Institute of Engineers in Geodesy, Aerial Photography, and Cartography resulted in the establishment of reference geodetic networks on the most active Kamchatkan volcanoes, preliminary aerial photography of those objects, and the plotting of quality large-scale (between 1:2,000 and 1:20,000) topographic plans and maps. In doing so, the scientists formed the theoretical basis for the photogrammetric investigation of volcanoes [6].

For aerial photography, the scientists used USSR analogue aerial photogrammetric cameras and Carl Zeiss Jena phototheodolites. A Carl Zeiss Jena stereocomparator, a Romanovsky stereoprojector, and a coordinatograph were used for photogrammetric processing. In 1984, the Institute of Volcanology bought the most advanced equipment from Carl Zeiss Jena: a multipurpose processing device Stereometrograph-G, an automatic plotting table, a high-precision stereocomparator, a photogrammetric rectifier, a data logger, and a data storage unit, which allowed to accomplish nearly all the tasks related to the processing of aerial and ground-based images. This equipment was put into use in 1985 and was used for 23 years, until 2008.

The quantitative characteristics were mathematically calculated using the results from Stereometrograph-G and the stereocomparator with the help of software made by N. F. Dobrynin at the Institute of Volcanology [7].

The 1973–2008 photogrammetric investigations on Kamchatka allowed for detailed research on morphodynamics and for the calculation of the quantitative characteristics of the 1975–1976 Great Tolbachik Fissure Eruption (GTFE) [8]. They also helped to determine the formation of Novy Dome on Bezymianny Volcano in 1976–1981 and a dome on Molodoy Shiveluch Volcano in 1980–1981 and 1993–1995 [9, 10]. Large-scale topographic maps and plans for the majority of the active Kamchatkan volcanoes were plotted during that period. For the first time, the morphological precursors of activation were revealed for the most frequently surveyed volcanoes, including Klyuchevskoy, Shiveluch, Bezymianny, and Maly Semyachik Volcanoes [11]. In addition, the scientists conducted an assessment of volcanic hazard posed by the Klyuchevskoy group of volcanoes and Avachinsky Volcano.

3.4. Digital stereophotogrammetry from 2008 to the present

Digital techniques were gradually introduced for the photogrammetric investigation of Kamchatkan volcanoes from the late 1990s onward. However, the Laboratory of Geodesy and Remote Sensing at the Institute of Volcanology and Seismology entirely shifted to the digital methods of photogrammetric investigation in 2008 with the purchase of the stereophotogrammetric software Photomod 4.3 by Racurs Company. This software can be substituted for the above-described optomechanical instruments.

The processing of images using Photomod 4.3 results in vector DTMs based on a triangulated irregular network. Quality of stereo modelling is estimated automatically in Photomod 4.3 after the exterior orientation.

http://dx.doi.org/10.5772/63577

The calculation of quantitative characteristics of eruptions, mapping, and 3-D modelling are based on the results from digital photogrammetric processing using Photomod 4.3, followed by more processing with the Surfer 10 software. The volumes of the volcanic edifices and of their elements are determined by subtracting the base DTM of the pre-eruptive terrain from the DTM tied to the date of survey. The volume calculating error is usually less than 1%.

Digital photogrammetric techniques were used for the investigation of the 2001–2012 Shiveluch eruption [12], the 2010–2012 Kizimen eruption [13], the 2012–2013 Tolbachik Fissure Eruption [14], and for other Kamchatkan volcanic and hydrothermal objects [15, 16]. Thus, the investigations resulted in detailed topographic maps of the abovementioned objects, their precise morphometric characteristics and, in particular, the detailed description of the impact from the Kizimen eruption and an assessment of hazard posed by Molodoy Shiveluch [17].

4. Some examples of studied active volcanoes

This part contains data on several volcanoes in Kamchatka that have been studied using the photogrammetric method (**Figure 3**). Objects with various types of activity were chosen to demonstrate that this method is universal.

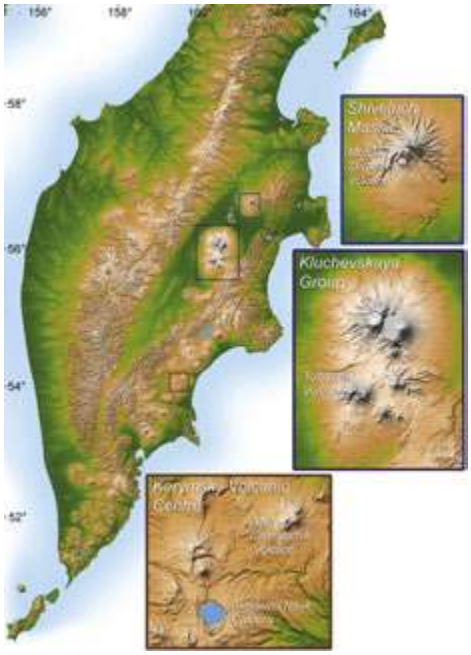

Figure 3. Map of the Kamchatka Peninsula showing the locations of the studied volcanic objects.

4.1. The growth of the Molodoy Shiveluch volcano dome

Molodoy Shiveluch volcano is located in the southwestern part of the Pleistocene Shiveluch massif (**Figure 4**) at a junction of the Aleutian and Kamchatkan volcanic arcs. The coordinates of the highest point of Molodoy Shiveluch are 56°38′10 N, 161°18′54 E, and its height is 2763 m. The volcanic edifice was comprised of several lava domes. The November 12, 1964, eruption resulted in their collapse and the 1.8 × 3.5 km double avalanche caldera formation [18]. The new lava dome has had three periods of steady growth: from 1980 to 1981, from 1993 to 1995, and now it has been growing since 2001.

Figure 4. View of the Shiveluch massif from the south in 2012.

Photogrammetric monitoring of the Molodoy Shiveluch caldera has been carried out since 1979. The investigation of the caldera surface using the 1980 models revealed that the 15-year hot lakes in the active crater on the caldera floor had already disappeared by July 3, 1980. Vertical deformations up to 3 m and a system of fractures were also revealed. The largest fracture was up to 2 × 55 m in size. The lakes' disappearance possibly resulted from the formation of fractures or from the heat flux increase in the area of the future dome formation. Hence, the disappearance of the lakes and the deformations of the caldera's active area surface were precursors to the lava dome's growth [11].

The investigation of the 1980–1981 and 1993–1995 periods, which was performed using instrumental photogrammetric survey, and of the 2001–2012 period, which was performed using a digital photogrammetric survey, allowed for the detailed monitoring of the dome's morphodynamics and revealed its quantitative characteristics.

During the 1980–1981 period, the lava dome reached the height of 185 m and became 0.02 km^3 in volume [9]. During the 1993–1995 eruption, the height of the dome reached 346 m, and its volume was estimated to be 0.2 km^3 [10]. The average lava output over the first two periods was estimated at 41,000 m^3/day and 280,000 m^3/day, respectively. In 1980–1981 and 1993–1995, the dome's growth was endogenous.

http://dx.doi.org/10.5772/63577

From 2001 to the present, the dome has mainly shown exogenous growth. In different parts of the dome, crease structures and lava lobes have formed and occasionally collapsed due to explosions and gravity.

In 2003, there was an inverse change in the type of the dome growth from exogenous to endogenous. Three lava plugs were formed in the western part of the dome (**Figure 5a**). The growth of the lava plugs resulted in the collapse of lava lobes that had covered the dome in 2002. There remained only a part of the northwestern lobe. Multiple avalanche chutes were formed on the southwestern flank of the dome. The relative height of the dome reached 499 m, and the volume reached 0.47 km^3.

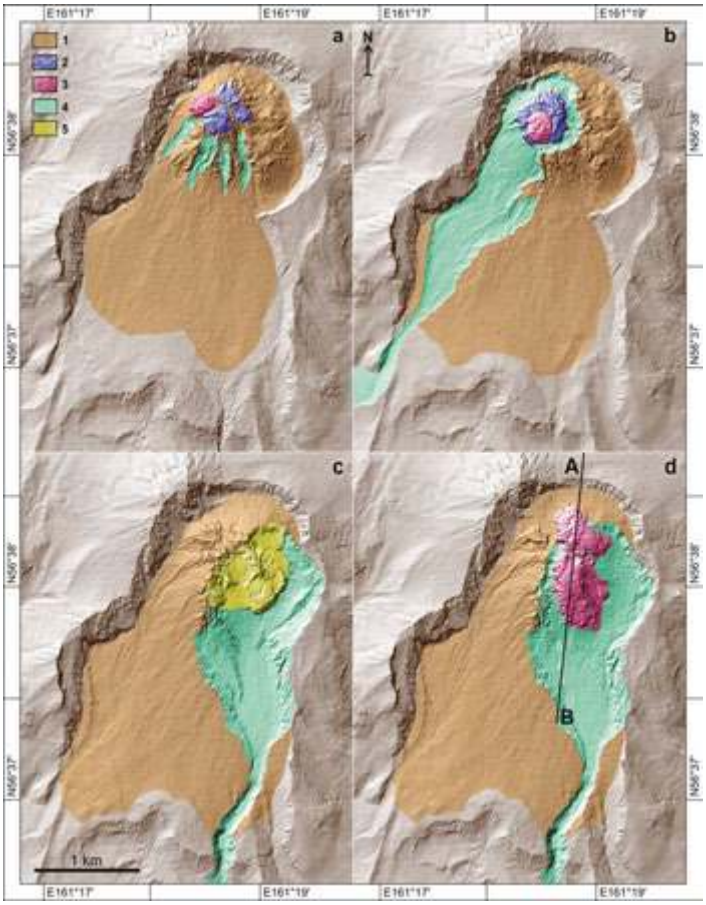

Figure 5. DTMs of the Molodoy Shiveluch caldera: a—October 7, 2003, b—August 21, 2005, c—November 22, 2010, d—July 12, 2012; 1—Dome with a talus mantle, 2—Endogenous lava units, 3—Exogenous lava units, 4—Negative landforms from collapses and explosions, 5—Inner part of the dome. The A–B line denotes the location of profiles shown in **Figure 6**.

We processed R. L. Wessels's images [19] using the photogrammetric method to reveal the state of the lava dome in 2005. It was found that the 2005 dome had been formed in several stages. The February 27, 2005, eruption resulted in a complex crater 730 m in diameter, a sector collapse of the dome, a Merapi-type pyroclastic flow, and the formation of an avalanche chute 620 × 2500 m in size (**Figure 5b**). The volume of the collapsed material was estimated at not less than 0.11 km^3. Then, a relatively small endogenous dome grew up inside the crater. An explosive funnel 280 m in diameter was formed in its southwestern sector. After that, round shape 55 m high and 270 m in diameter lava lobe with prominent crease structure on the surface was extruded from the funnel. The polygenetic dome's relative height was 484 m. Its volume was estimated at 0.48 km^3.

On October 27, 2010, another large sector collapse of the dome edifice occurred at Molodoy Shiveluch. It resulted in the outcrop of an inner part of the dome and the formation of an avalanche chute 1084 × 2455 m in maximum size (**Figure 5c**). The volume of the collapsed material was 0.28 km^3. After the collapse, the relative height of the dome was 557 m, and the volume was estimated to reach 0.54 km^3.

In 2012, the exogenous dome continued to grow (**Figure 5d**). A blocky lava lobe 385 × 755 m in maximum size was formed on its southern flank. A large explosive crater 60 m deep and 150 m in diameter was revealed at the top of the lobe. By July 12, 2012, the extrusive activity centre at Molodoy Shiveluch Volcano had moved to the northern flank of the dome. The new lava lobe of the northern centre was 450 × 590 m in size. Its scoriaceous surface was bisected by a 6 × 470 m fracture. In its uppermost part, the extrusion of ductile material formed a crease structure 160 × 210 m in maximum size. The relative height of the dome was 526 m, and the volume was 0.63 km^3. The average lava discharge in the 2001–2012 period exceeded 225,000 m^3/day [12].

Figure 6 shows profiles of the topographic alteration of the dome morphology during the 2001–2012 period as compared with the previous 1980–1981 and 1993–1995 periods. The July 12, 2012, cross-section of the dome shows that the migration of eruptive centres and the piling up of lava lobes on its surface caused its irregular shape. While the October 1, 1994, and October 22, 1980, cross-sections of the dome agree with its morphology of a classical endogenous type.

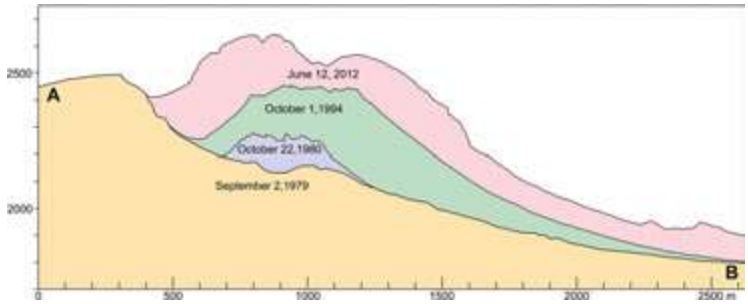

Figure 6. Profiles of the Molodoy Shiveluch lava dome. The A–B profile line location is shown in **Figure 5d**.

http://dx.doi.org/10.5772/63577

4.2. Tolbachik fissure eruptions

The doubled cone of the coalescing Ostry Tolbachik (55°49′50 N, 160°19′30 E) and Plosky Tolbachik volcanoes are located in the southwestern sector of the Klyuchevskaya group of volcanoes (**Figure 7**). Although these volcanoes' edifices were formed simultaneously in the Late Pleistocene [20], only Plosky Tolbachik Volcano was active in the Holocene. Additionally, not only were there summit eruptions, but there were also lateral eruptions from a large fissure zone that begins about 30 km to the south-southwest of the volcano, goes directly to its top, and continues about 10 km to the northeast of it. Historical eruptions occurred only in the south-southwestern part of the fissure zone in the territory known as Tolbachik Dale.

Figure 7. View of 2012–2013 Tolbachik Fissure Eruption from the north in 2012.

The largest and best-studied historical eruptions are the 1975–1976 Great Tolbachik Fissure Eruption (GTFE) and the 2012–2013 Tolbachik Fissure Eruption (TFE). Both eruptions were studied using aerial photogrammetric survey. From 1975 to 1977, aerial surveys of GTFE were carried out four times; archival aerial photographs from 1950 to 1974 were also used.

Photogrammetric processing resulted in the creation of maps and the obtaining of accurate data on the volume of terrain variations such as new lava fields, cinder cones, pyroclastic deposits, and subsidence effects in the summit pit crater of Plosky Tolbachik Volcano [8, 20].

From 2012 to 2013, the 2012–2013 TFE was investigated three times using aerial photography; we also used the 1987 archival aerial photos and the EO-1 satellite image from March 6, 2013. As the result of the 2012–2013 TFE images processing, we obtained DTMs, maps, and quantitative morphometric data. The analysis of the obtained data as well as the initial aerial images of the two eruptions allowed us to reveal their similarities and differences.

GTFE (**Figure 8**) consisted of two stages: Northern Breakthrough (from July 6 to September 15, 1975) and Southern Breakthrough (from September 15, 1975 to December 10, 1976). At that, eruptive centres appeared subsequently both in space and time and in rather short surface fissures (200–600 m), migrating first in the area of the Northern Breakthrough from the southwest to the northeast and then locally in the area of the Southern Breakthrough.

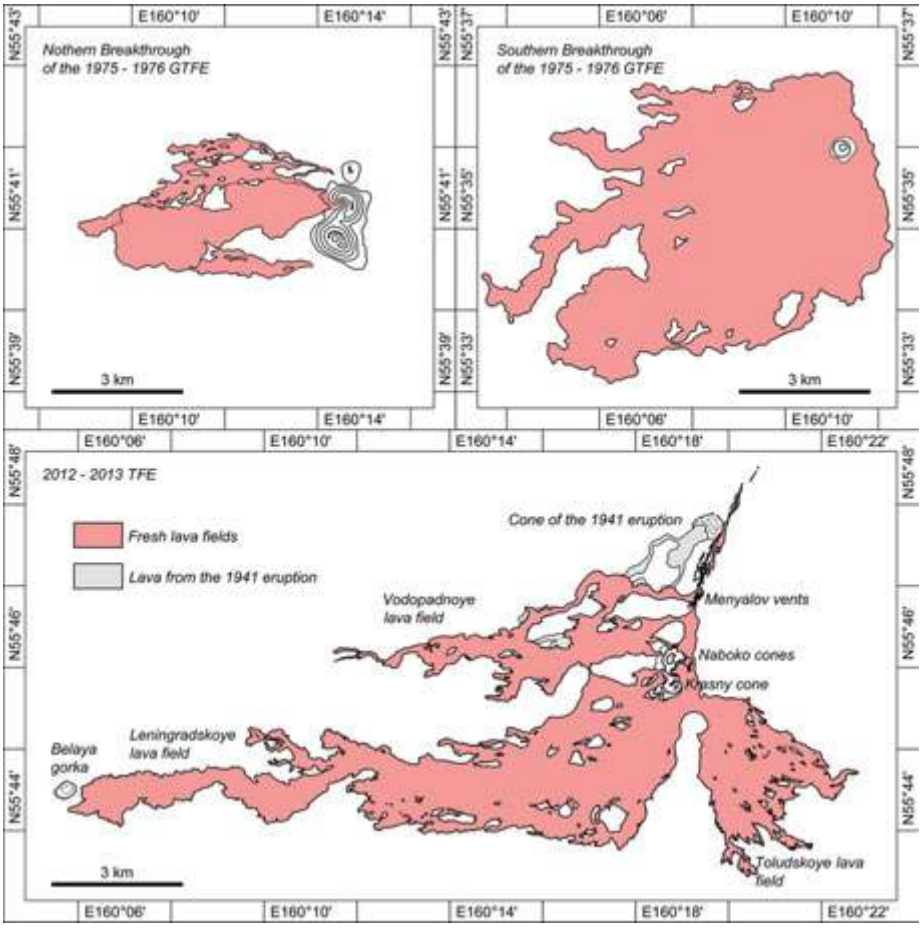

Figure 8. Maps of lava fields of the 1975–1976 Great Tolbachik Fissure Eruption and the 2012–2013 Tolbachik Fissure Eruption.

The eruption was preceded by a long build-up period and manifested in the activity of the summit pit crater of Plosky Tolbachik Volcano. During the period of 1967–1970 a lava lake, lava fountains, and the gas and steam emissions periodically appeared in it. After a 4-year period of repose from 1970 to 1974, the gas and steam emissions resumed and the ash and Pele's hair ejecta started 8 days prior to the eruption.

http://dx.doi.org/10.5772/63577

GTFE resulted in significant subsidence and collapses in the summit pit crater of Plosky Tolbachik volcano. In 1974, the volume of the well-shaped pit crater was estimated to be 0.02 km^3, and by the end of the eruption (1976), its volume increased to 0.35 km^3.

The eruption of Northern Breakthrough during GTFE was mainly explosive and resulted in the formation of cinder cones up to 300 m high. The volume of the cones and the adjacent area's pyroclastics was about 0.5 km^3. The volume of lava flows covering the 8.86 km^2 area reached 0.22 km^3. The eruption of Southern Breakthrough during GTFE was completely effusive and lasted 15 months. This resulted in the formation of lava flows 0.97 km^3 in volume that covered the 35.87 km^2 area and a small cinder cone that was 165 m high with a volume of 0.01 km^3 [8].

The 2012–2013 Tolbachik Fissure Eruption (**Figure 7**) started quite unexpectedly. Its fissure zone was over 5 km long and formed almost instantly. At first, a lot of explosive-effusive vents was erupting simultaneously within the whole fissure zone.

This eruption was mainly effusive. The rate of lava discharge to the surface during the first 2 days was 440 m^3/s, which was much greater than the rate of solid material discharge over the same period of time during the formation of the first GTFE's cinder cone in 1975.

However, by June 5, 2013, the area of the 2012–2013 TFE's lava fields, which was 35.23 km^2, nearly coincided with the area of GTFE's Southern Breakthrough, but the volume of lava was twice smaller and reached 0.52 km^3, which could be explained by the large slope angle of the underlying surface in the new eruption area. Furthermore, a lot of small cinder formations up to 15 m high and a group of Naboko cones up to 123 m high with a total volume of 0.02 km^3 were formed during the 2012–2013 TFE around the vents of the fissure zone [14].

The summit pit crater of Plosky Tolbachik Volcano was not involved during the 2012–2013 TFE. We only noted the very slight crumbling of the 1975–1976 pit crater's northwest walls. This crumbling was not associated with the eruptive activity and occurred under the influence of gravity.

4.3. Morphodynamics of Troitsky crater on Maly Semyachik volcano

Maly Semyachik volcano is a part of the Karymskaya group of volcanoes. It is located to the south of the central zone of the Eastern Kamchatkan volcanic belt. The coordinates of the active crater centre are 54°07′06″N and 159°39′20″ E. The volcano edifice is a 3-km-long ridge formed at the junction of three subsequently formed volcanic cones. Today, the active crater is Troitsky, which is located in the southwestern cone. One of the most acidic (pH varies from 0.5 to 0.75 [21]) volcanic lakes in the world Zelyonoe Lake is located in the crater.

Though Maly Semyachik was a common object of investigation, certain peculiarities were only revealed during systematic aerial photography, which has been conducted by the Institute of Volcanology since 1974.

For the first time, aerial photogrammetric surveys proved successful during the investigation of this volcano in 1986. The images from June 2, 1986, showed distinct concentric turbid spots on the surface of Zelyonoe Lake (**Figure 9**). The size of the spots varied from image to image within one aerial pass, which is evidence for the rapid movement of water masses in this part

of the lake [11]. This fact indicated an ongoing eruption, which was proven during the fieldwork in August–September 1986. Scientists detected increased water temperature as well as rapid gas emissions and other components of volcanic origin from the vent on the lake bed beneath the turbid spot [22].

Figure 9. Zelyonoe Lake in Troitsky Crater of Maly Semyachik Volcano in 1986 from the southwest.

Further photogrammetric investigation of new and archival photos allowed for the detailed morphodynamic analysis of Troitsky Crater and Zelyonoe Lake during the 1946–2012 period, the estimation of the lake level and the crater shape, and these data relation to data from previous fieldwork.

Aerial photography revealed a considerable fall in water level over the 1946–1950 period. During that period of time, the morphology of the crater significantly changed: a negative landform appeared in the northeastern sector of the crater's lake shore. It was 200 m in diameter and had a gentle bottom profile. Its steep sides were as high as 50 m.

Though this negative landform was supposed to have an explosive nature [23], the 1950 images showed no traces of tsunami in the lake. Additionally, the appearance of this landform only caused a minor migration of fumarole gas emission near it and had no effect on the fumarole regime. Thus, this form most likely appeared due to gravity. The results from the photogrammetric measurements showed that the lake area increased by 8000 m^2 (for the 1138 m level). The crater reshaping and the fall in water level could have had a cause-and-effect relationship in the case of increased subsurface discharge within the newly formed lake bed, which is composed of permeable rocks that are unaltered by contact with thermal acid solution.

http://dx.doi.org/10.5772/63577

The analysis of the aerial photographs revealed constant landslides and crumbling on the inner walls of Troitsky Crater, the material that enters the lake, affecting its bed morphology and thus its surface level. The volumes of the above-water part of the crater for 1968 and 2012 toward one plane related to a higher level in 2012 were estimated to be 91,000,000 m^3 and 92,500,000 m^3, respectively. The difference in volumes is 1,500,000 m^3, which is the scree material deposited on the bottom of the crater during the last 44 years. Over the 1968–2012 period, the water level rose from 1139.1 to 1176.3 m, and thus increased by 37.2 m. The volume gain was estimated to be 9,000,000 m^3. Therefore, the bulk of scree material for 44 years accounts for 17% of the lake volume gain. With respect to the friability of the rocks that crumbled from the crater walls, the contribution of screes to the volume gain of water should be reduced to no less than 10%. Thus, when evaluating the dynamics of the lake depth, it is important to include the material that crumbled into the lake water over the entire period of investigation along with the feeding and discharge processes [16].

Based on the results of the photogrammetric processing of aerial photographs from various years, we plotted maps for 1950 and 2012 (**Figure 10**) and created crater profiles for 1950, 1968, and 2012 (**Figure 11**). Additionally, a graph of the lake water level for the period from 1946 to 2012 was plotted (**Figure 12**). The graph shows that the moderate increase of the water level —0.9 m per year—since 1950 has been accompanied by the rapid increase of the water level related to volcanic unrest. Over the 1968–1971 period, the water level rose by 13 m, and over the 1981–1986 period, it rose 8.7 m higher. According to the complex investigation [22, 24], the above periods were periods of high activity, which manifested in the maximum temperature of the lake water.

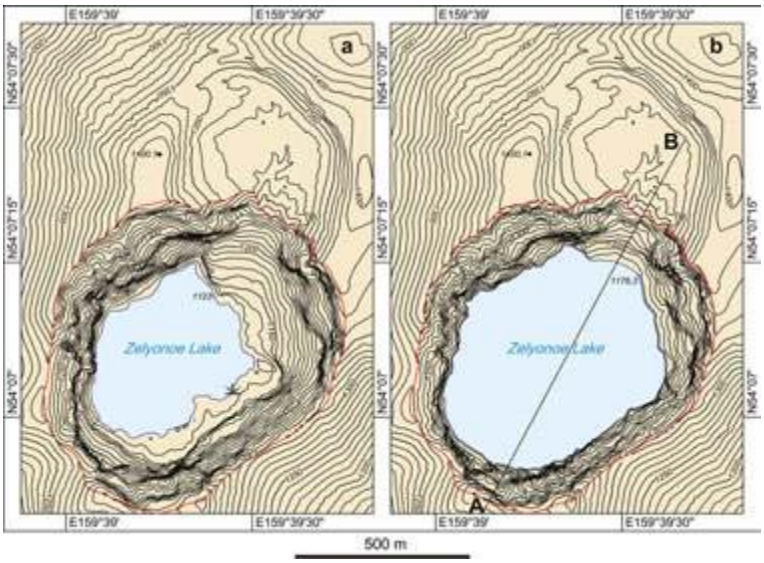

Figure 10. Maps of Troitsky Crater: a—1950, b—2012. The A–B line denotes the location of profiles shown in **Figure 11**.

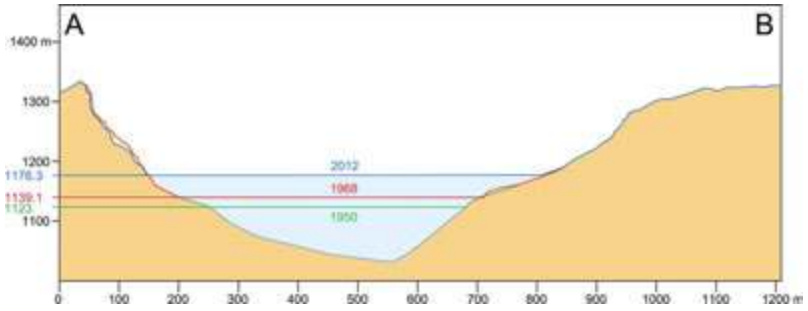

Figure 11. Profiles of Troitsky Crater in 1950, 1968, and 2012. The position of the A–B line is shown in **Figure 10b**.

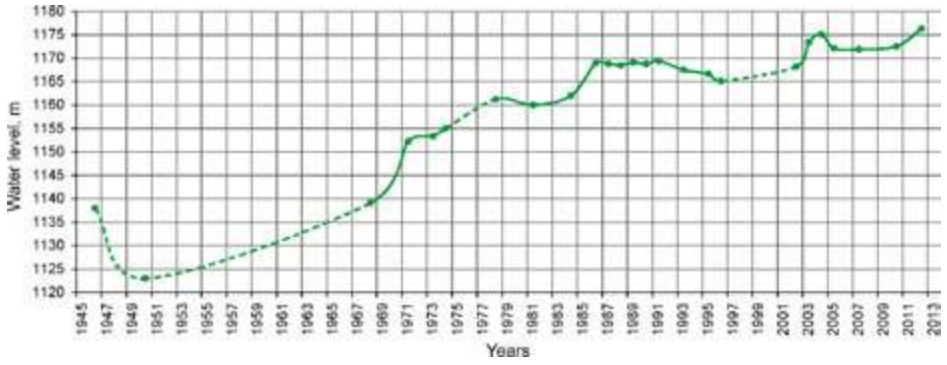

Figure 12. Graph of the Zelyonoe Lake water level over the period 1946–2012. The dotted line denotes the zones with at least 4-year-long pauses between monitoring.

4.4. Catastrophic eruption in Akademii Nauk Caldera

Akademii Nauk Caldera is located in the Karymsky Volcanic Centre 30 km from the eastern coast of Kamchatka. The coordinates of the caldera centre are 53°59′00″ N and 159°27′40″ E. The major part of the caldera contains Karymskoye Lake, which is one of the largest volcanic lakes in Kamchatka. The lake's middiameter is 3.7 km, and it is as deep as 70 m and occupies an area of 10.3 km^2. There are many thermal springs inside the lake and on its shore, including some geysers on its southeastern shore. The caldera had been supposed to be volcanically inactive until 1996.

On January 1, 1996, a swarm of shallow earthquakes with magnitudes up to 6.9 was detected within the Karymsky Volcanic Centre. That is the highest crust magnitude that has ever been detected in the history of seismological survey in Kamchatka [25]. The seismic event caused the simultaneous eruption of Karymsky Volcano and Akademii Nauk Caldera (**Figure 13**). The eruption in Akademii Nauk Caldera was short and lasted from 2 to 3 p.m. on January 2 to 11 a.m. on January 3 [26], yet it caused significant consequences:

http://dx.doi.org/10.5772/63577

1. A new crater called Tokarev appeared, resulting in the formation of the Novogodny Peninsula in the northern sector of Karymskoe Lake;
2. The lake shore and bed terrain was changed;
3. A tsunami washed out the once steep and overgrown shore;
4. The head of the Karymskaya River was blocked by erupted material, resulting in a lake dam, but on May 16, 1996, the dam was washed out and a flood rushed into Vulkanostantsiya Valley, deluging it for several hours.

Figure 13. The January 2, 1996, eruption in Akademii Nauk Caldera.

The events on January 1–3, 1996, caused ground cracks of submeridional trend and gaps within a 2×0.5 km area stretching from Tokarev Crater to a lava field near Lagerny Cone. Cracks and small maars were also formed on the surface of Novogodny Peninsula. The eruption caused new groups of thermal springs on the northern shore of Karymskoye Lake and on the rim of Tokarev Crater.

The changes caused by the events were studied using aerial photogrammetry. The Karymsky Volcanic Centre had been studied in detail before these events. There is a geodetic network with numerous ground control points within the volcanic centre that have been used since 1973 and have contributed greatly to the geodetic adjustment for photogrammetric models. The area of the events (the northern part of Karymskoye Lake) has been shot using aerial photography since 1978. In order to evaluate the impact of the events, we used images from the 1984 survey. The impact was investigated and mapped based on materials from several aerial surveys for certain years (1996, 2000, and 2003).

The aerial photographs and their photogrammetric processing contributed to detailed maps prior to and after the events of January 1–3, 1996 (**Figure 14**). The alterations were revealed in detail despite the lack of previous volcanological investigation in the northern part of Karymskoye Lake. Thus, the aerial photographs showed that there are both new and old ground cracks within the studied area.

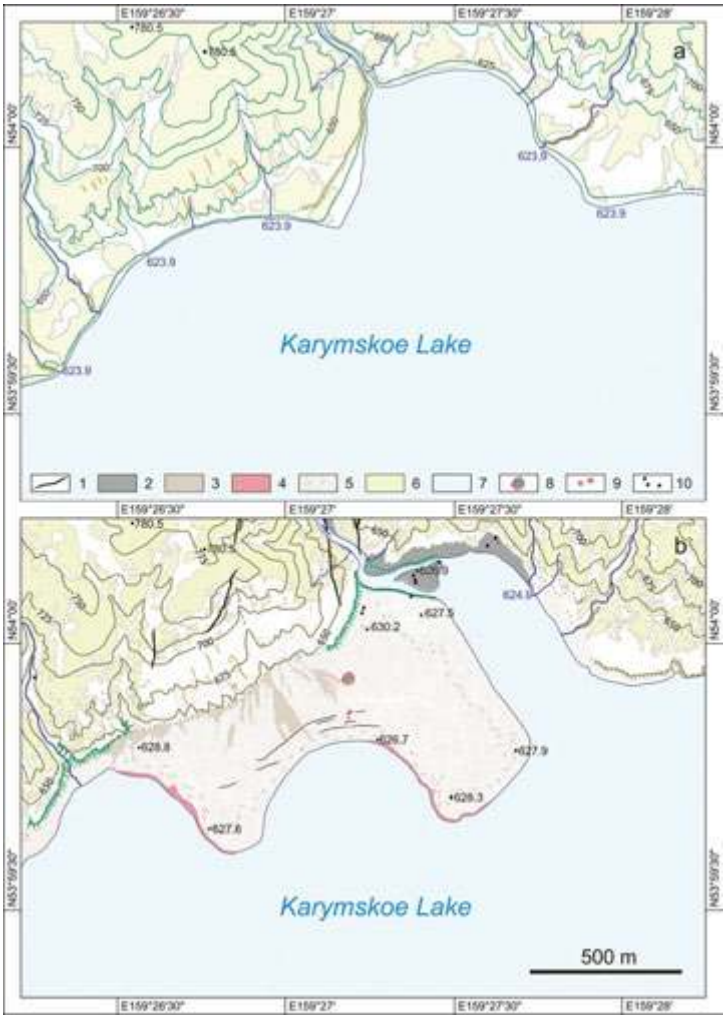

Figure 14. A map of northern sector of Akademii Nauk Caldera before (a) and after (b) the 1996 eruption: 1—Open-joint cracks caused by the 1996 event, 2—Deposits of the January–May 1996, mud flows, 3—Deposits of small mud flows in Novogodny Peninsula caused by the erosion of the shore cliff, 4—Heated zones, 5—Surface with destroyed vegetation or without it, 6—Forest cover, 7—Water surfaces, 8—Maar, 9—Explosion funnels and pit craters, 10—Large stones.

http://dx.doi.org/10.5772/63577

The stereo photogrammetric method helped to detect traces of tsunami waves on various sectors of the shore. The highest waves (50 m above water level) were detected in the northern sector of the lake, close to Novogodny Peninsula. The height of the waves on the outermost from Tokarev Crater southern sector of the lake was estimated to reach 10 m.

Mud deposits caused by the flood in Vulkanostantsiya Valley right after the dam washout covered the territory of 0.37 km^2 with an average thickness of 3 m.

Complex geodetic and photogrammetric investigation of Karymskoye Lake shore allowed for the creation of the first detailed topographic plans of thermal springs in Akademii Nauk Caldera. In addition to the coordinates of the springs, the tachymetry obtained the coordinates of the surface points where temperature was measured, which allowed for the precise definition of isotherms on those plans [27].

The investigation of the 1996 eruption in Akademii Nauk Caldera and of its impact showed that photogrammetry is an important, feasible, and universal method in volcanology and in the study of the local impacts of tsunamis and large seismic events. Materials from this work are not limited to the maps because the DTM plotted using these results may become the basis for the modelling of seismotectonic and tsunami-causing processes.

5. Conclusion

In the context of the investigation of active Kamchatkan volcanoes, we can trace over more than a century of evolution in the photogrammetric method from 1908 to the present. Until the middle of the last century, scientists had to expand their efforts to conduct ground-based photogrammetry. In 1946, aerial methods were introduced that provided more opportunities, yet photogrammetry was not used in full due to the lack of geodetic adjustment. Full-scale stereo photogrammetric investigations became available in the 1970s and 1980s with the introduction of advanced instruments and preparatory geodetic work at the studied objects. Later, digital technologies helped to facilitate image processing and reduced the time required to perform the operations. Additionally, the improvements in the software made it possible to obtain high-quality supporting materials (maps and 3-D models), which provided informative data on the studied volcanoes based on the results from photogrammetric processing.

It is necessary to notice that for the first time ever in volcanological research, the photogrammetric method was used in Kamchatka (1908–1910), and after that it was used in the 1940s for the study of the Paricutin Volcano eruption in Mexico [28]. Today, this method is used for the study of the morphology and morphodynamics of volcanoes all over the world, along with such remote sensing methods as interferometry and laser scanning.

The evolution of surveying instruments and computers makes the photogrammetric method ever more actual. Digital technology makes both surveying and photogrammetric processing much cheaper. New surveying instruments have been developed such as unmanned aerial vehicles and satellites equipped with high-resolution stereo cameras.

Algorithms for the photogrammetric processing of images have also been improved. One of the advanced developments is, we think, a pixel-to-pixel matching method that is capable of finding on stereo models a pair for each pixel of each image using a mathematical approach [29]. Computing capabilities of modern computers allow for detailed image analysis in order to reconstruct the shape of the studied object precisely (**Figure 15**).

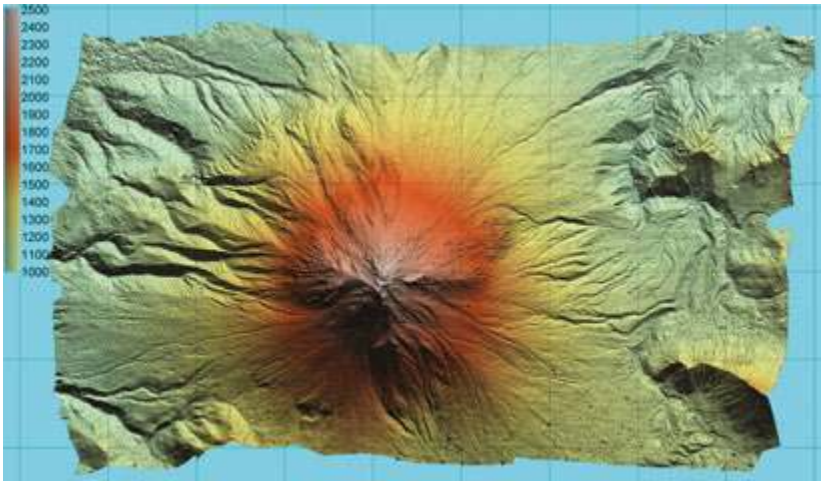

Figure 15. DTM of Kizimen Volcano made by independent programmer Andrey Matseevsky using the pixel-to-pixel matching method. Zones with weak correlation are smoothed.

We hope that the examples and information provided in this chapter will help to understand how to use the instrumental and scientific capabilities of images as well as how to advance photogrammetric investigation in volcanology.

Acknowledgements

The authors would like to express gratitude to Andrey Matseevsky for providing us with the DTM of Kizimen Volcano, and Dmitry Isaev and Ekaterina Minakova for assisting us with the translation.

Author details

Viktor Dvigalo*, Alina Shevchenko and Ilya Svirid

*Address all correspondence to: dvig@kscnet.ru

Institute of Volcanology and Seismology FEB RAS, Petropavlovsk-Kamchatsky, Russia

References

[1] Mikhail EM, Bethel JS, McGlone JC. Introduction to Modern Photogrammetry. New York: John Wiley & Sons Inc.; 2001. pp. 496.

[2] Dvigalo VN, Svirid IY, Shevchenko AV. The revival of the lost collection of photographic plates of the geological department of the F.P. Ryabushinsky's Expedition to Kamchatka, 1908–1910. Voprosy Geografii Kamchatki. 2008; 12: 87–98.

[3] Kell NG. Map of the Volcanoes of Kamchatka. Leningrad: Russian Geographical Society; 1928. 76 pp.

[4] Konrady SA, Kell NG. The geological department of the 1908–1910 expedition to Kamchatka. Izvestiya GRGO. 1925;57:3–32.

[5] Dobrokhotov YS. Aerial survey in volcanological expeditions of the USSR Academy of Sciences. Priroda. 1951;12:12–19.

[6] Gusev NA, Dobrynin NF. The theoretical grounds of the aerophotogrammetric method in volcanology. Vulkanologiya i Seismologiya. 1979;(5): 50–61.

[7] Fedotov SA, Dobrynin NF, Dvigalo VN. Analytical-photogrammetric system for quantitative evaluation of the volcanos activity. Geodeziya i Kartografiya. 1989;(1): 22–29.

[8] Fedotov SA, editor. Bol'shoe treshchinnoe Tolbachinskoe izverzhenie, 1975–1976 gg. [The 1975–1976 Great Fissure Tolbachik Eruption]. Kamchatka. Moscow: Nauka; 1984. pp. 640.

[9] Dvigalo VN. Growth of a dome in the crater of Shiveluch Volcano in 1980–1981 from photogrammetry data. Volcanol. Seismol. 1988;6:307–315.

[10] Melekestsev IV, Dvigalo VN, Kirsanova TP, Ponomareva VV, Pevzner MM. The 300 years of Kamchatka volcanoes: the Young Shiveluch. An analysis of the dynamics and impact of eruptive activity during the 17–20th centuries. Part II. 1965–2000. Vulkanologiya i seismologiya. 2004;(1):5–24.

[11] Dvigalo VN. Morphological precursors (first indications) of volcanic eruptions in Kamchatka. Volcanol. Seismol. 2000;22:351–369.

[12] Shevchenko AV, Dvigalo VN, Svirid IY. Airborne photogrammetry and geomorphological analysis of the 2001–2012 exogenous dome growth at Molodoy Shiveluch Volcano, Kamchatka. J. Volcanol. Geotherm. Res. 2015;304:94–107. DOI: 10.1016/j.jvolgeores.2015.08.013.

[13] Dvigalo VN, Melekestsev IV, Shevchenko AV, Svirid IY. The 2010–2012 eruption of Kizimen Volcano: the greatest output (from the data of remote sensing observations) for eruptions in Kamchatka in the early 21st century. Part I. The November 11, 2010 to

December 11, 2011 phase. J. Volcanol. Seismol. 2013;7:345–361. DOI: 10.1134/S074204631306002X.

[14] Dvigalo VN, Svirid IY, Shevchenko AV. The first quantitative estimates of parameters for the Tolbachik fissure eruption of 2012–2013 from Aerophotogrammetric observations. J. Volcanol. Seismol. 2014; 8: 261–268. DOI: 10.1134/S0742046314050029.

[15] Dvigalo VN, Melekestsev IV. The geological and geomorphic impact of catastrophic landslides in the Geyser valley of Kamchatka: Aerial photogrammetry. J. Volcanol. Seismol. 2009;3:314–325. DOI: 10.1134/S0742046309050029.

[16] Svirid IY, Shevchenko AV, Dvigalo VN. Investigation of Maly Semyachik Volcano (Kamchatka) activity using morphodynamic data from the Troitsky crater. Vestnik KRAUNTs. Nauki o Zemle. 2013;22:129–143.

[17] Shevchenko AV, Svirid IY. Hazard assessment for Molodoy Shiveluch Volcano from geomorphologic interpretation and photogrammetric processing of stereo photo- and satellite images. In: Proceedings of the VII Schukin conference on Geomorphological resources and geomorphological safety: from theory to practice; 18–21 May 2015; Moscow. Moscow: MSU; 2015. pp 206–209.

[18] Melekestsev IV, Volynets ON, Yermakov VA, Kirsanova TP, Masurenkov YP. Sheveluch Volcano. In: Fedotov SA, Masurenkov YP, editors. Active Volcanoes of Kamchatka. Vol. 1. Moscow: Nauka; 1991. pp. 82–103.

[19] Ramsey MS, Wessels RL, Anderson SW. Surface textures and dynamics of the 2005 lava dome at Shiveluch Volcano, Kamchatka. GSA Bull. 2012; 124: 678–689. DOI:10.1130/B30580.1.

[20] Dvigalo VN, Fedotov SA, Chirkov AM. Plosky Tolbachik. In: Fedotov SA, Masurenkov YP, editors. Active Volcanoes of Kamchatka. Vol. 1. Moscow: Nauka; 1991. pp. 198–211.

[21] Selyangin OB, Braitseva OA. Maly Semiachik Volcano. In: Fedotov SA, Masurenkov YP, editors. Active Volcanoes of Kamchatka. Vol. 2. Moscow: Nauka; 1991. pp. 160–179.

[22] Gavrilenko GM, Dvigalo VN, Fazlullin SM, Ivanov VV. The present-day state of Malyi Semyachik Volcano, Kamchatka. Volcanol. Seismol. 1993;15:129–135.

[23] Slezin YB, Kovalev GN, Grebzdy EI, Chegletsova EA. On activity of Maly Semiachic Volcano. Byulleten Vulkanologicheskih Stantsyi. 1971;47:37–39.

[24] Dvigalo VN, Andreev VI, Gavrilenko GM, Ovsyannikov AA, Razina AA, Chirkov AM. Activity of the southeast Kamchatka and north Kuriles volcanoes in 1985–1986. Volcanol. Seismol. 1990;10:347–359.

[25] Fedotov SA. Study and mechanism of the simultaneous 1996 Karymsky Volcano and Akademii Nauk Caldera eruptions in Kamchatka. Volcanol. Seismol. 1998;19:525–566.

[26] Fazlullin SM, Ushakov SV, Shuvalov RA, Aoki M, Nikolaeva AG, Lupikina EG. Underwater eruption in the Akademii Nauk Caldera, Kamchatka, and its consequences: Implications from hydrogeological, hydrochemical and hydrobiological studies. Volcanol. Seismol. 2001; 22:375–395.

[27] Karpov GA, Dvigalo VN. Thermal discharge in the caldera of Akademii Nauk: results of topographic and hydrologic surveys of thermal springs after the 1996 catastrophic submarine eruption. In: Proceedings of the Regional conference on Volcanism and associated processes; 30–31 March 2009; Petropavlovsk-Kamchatsky. Petropavlovsk-Kamchatsky: Institute of Volcanology and Seismology FEB RAS; 2009. pp. 101–114.

[28] Flores-Covarrubias L. Calculos para la determinacion de la altura del cono del volcan del Paricutin. [Calculations for determining the height of the Paricutin cone] In: Flores T, editor. El Paricutin. Estado de Michoacan. Mexico: Universidad Nacional Autonoma de Mexico. Instituto de Geologia; 1945. p. 19–20.

[29] Yaguchi Y, Iseki K, Oka R. Optimal pixel matching between images. In: Wada T, Huang F, Lin S, editors. Advances in Image and Video Technology. PSIVT 2009; 13–16 January 2009; Tokyo. Berlin: Springer-Verlag; 2009. pp. 597–610.